Research on Chemical Intermediates (2019) 45:1105–1116
https://doi.org/10.1007/s11164-018-3666-8

Phyto-synthesis of silver nanoparticles using aerial extract of *Salvia leriifolia* Benth and evaluation of their antibacterial and photo-catalytic properties

Mohammad Ehsan Taghavizadeh Yazdi[1] · Masoomeh Modarres[2] · Mohammad Sadegh Amiri[3] · Majid Darroudi[4,5]

Received: 10 August 2018 / Accepted: 8 November 2018 / Published online: 15 November 2018
© Springer Nature B.V. 2018

Abstract

We have synthesized silver nanoparticles (Ag-NPs) via a simple and eco-friendly method through the utilization of aqueous aerial parts of *Salvia leriifolia* Benth. The formation of Ag-NPs was indicated by varying the observed colors towards dark red. The biosynthesized Ag-NPs were characterized with diverse instrumental tools, e.g., UV–Vis, XRD, FESEM, EDX, TEM, and FTIR. As for the results, Ag-NPs formation using silver nitrate (1.0 mM) led to the development of EMly shaped nanoparticles with a mean diameter of about 12.7 nm. Moreover, the green synthesized Ag-NPs seemed to demonstrate a higher antibacterial activity in opposition to pathogenic bacteria (*Staphylococcus aureus*, *Bacillus subtilis, Escherichia coli* and *Pseudomonas aeruginosa*). Maximum inhibition zone belonged to *E. coli* with 10.5 mm. Also, biosynthesized Ag-NPs seem to contain satisfying photocatalytic activity against stable organic compound (i.e., Methylene Blue). This process may be extended for the vast scale preparation of metal nanoparticles for various industrial applications.

Keywords Silver nanoparticles · Antibacterial · Photo catalyst · *Salvia leriifolia* Benth

✉ Majid Darroudi
darroudim@mums.ac.ir; majiddarroudi@gmail.com

[1] Nanotechnology Research Center, Pharmaceutical Technology Institute, Mashhad University of Medical Sciences, Mashhad, Iran

[2] Department of Biology, Faculty of Science, Farhangian University of Khorasan Razavi, Mashhad, Iran

[3] Department of Biology, Payame Noor University, Tehran, Iran

[4] Nuclear Medicine Research Center, Mashhad University of Medical Sciences, Mashhad, Iran

[5] Department of Modern Sciences and Technologies, Faculty of Medicine, Mashhad University of Medical Sciences, Mashhad, Iran

Introduction

Noble metal nanoparticles (e.g., Ag, Au, Pt) have attracted substantial attention from many fields including medicine [1–4], biotechnology [5, 6], materials science [7, 8], catalytic activity [9, 10], antimicrobial properties [11, 12], photonics, and electronics [13, 14]. The interest in nanoparticles have arisen from their size, shape and surface morphology that ultimately determines their chemical, physical, optical and electronic properties [15]. The chemical and physical techniques that are used to prepare nanoparticles often involve toxic materials and procedures that are not eco-friendly but quite expensive [16, 17]. On the other hand, methods that utilize biological ways to synthesize nanoparticles are green, eco-friendly and capable of overcoming most of the harmful effects produced by chemical and physical techniques. Since green chemistry methods employ biological systems such as plants and similar organisms, they stand as an attractive and fine substitute for physiochemical procedures [18–21]. The green-based biosynthesis approach has also the benefits of being a straightforward and eco-friendly process. The usage of plant extracts in synthesizing metallic nanoparticles has been extensively reported throughout literature [22–24]. Bioactive components that exist in the extracts play the roles of reducing and stabilizing factors. *Salvia leriifolia* Benth (Fig. 1) has been used as an expectorant, antipyrétique and laxative in the markets of Mashhad, Iran; while the aerial parts of *S. leriifolia* Benth., called "Nowruzak" in the Persian language, has been recognized as a hypoglycemic and period regulator [25, 26]. In this project, we have reported an innovative green way that is done at room temperature regarding the biosynthesis of Ag-NPs from $AgNO_3$ via the aerial extracts of *S. leriifolia* Benth.

Fig. 1 A photograph of *S. leriifolia* Benth

Materials and methods

Materials

Fresh aerial parts of *S. leriifolia* were collected from the Khorasan razavi province of Iran, and verified by Voucher specimen (No. 375) that was deposited in the Dargaz Payame Noor University Herbarium. Silver nitrate ($AgNO_3$, Pre-Analysis) was procured from Carlo Erba (France). The aerial parts of *S. leriifolia* were cleaned and dried during 4 days at ambient temperature.

Provision of aerial extract

The aerial parts of *S. leriifolia* were cleaned and dried during 4 days at ambient temperature. After that, the dried segments convert to powder with a blade grinder. Approximately 3.0 g of *S. leriifolia* dried powder (aerial parts) was transferred into a culture dish contained 300 ml of deionized water for 24 h. At the end, the extract was ready by filtered filtration through filter paper (Whatman #1).

Biosynthesis of silver nanoparticles

For the green-synthesis of Ag-NPs from aerial extract, 10 mL of extracts aerial parts were bit by bit added to 90 mL of $AgNO_3$ solution (1 mM), after that combination was dynamically motivated at room temperature. In order to eliminate the unreacted phytochemicals, the synthesized Ag-NPs were harvested by utilizing a centrifuge.

Characterization of biosynthesized silver nanoparticles

The biosynthesized Ag-NPs were characterized through a number of helpful techniques, including UV–vis (CECIL instrument CE 9500, UK), FESEM (FE-SEM, TESCAN, MIRA 3), EDX, TEM (Zeiss EM 10 C-100 kV, Germany), XRD (D8 ADVANCE-BRUKER, Scan rate = 1.0° min^{-1}) and FTIR (Shimadzu 8400, Japan), in a sort of (300–900 nm) scan that was performed via UV–Visible spectroscopy. The morphology and dimensions of the Ag-NPs were verified by employing a TEM and a FESEM machine. The crystalline construction of these particular nanoparticles was determined by the use of XRD. FTIR was utilized to stuff the efficient clusters in the biosynthesized Ag-NPs. Mashhad University of Medical sciences (MUMS) supported the instrumental techniques.

Antibacterial activity

The antibacterial investigation of Ag-NPs was assessed through the disk-diffusion method. Four bacterial strains named Gram-positive bacterial (*Staphylococcus aureus* and *Bacillus subtilis*) and Gram negative bacteria (*Escherichia coli* and

Pseudomonas aeruginosa) were obtained from Mashhad Medical Science, Mashhad, Iran. The surface of Muller Hinton Agar (MHA) was injected via the bacteria by rushing the swab and afterwards disks were soaked with 15 µL of Ag-NPs solution that were positioned on the injected agars [27]. The antibacterial action was created on the presence of an inhibition region nearby the disks.

Photo-catalytic activities

To experiment with the photo-catalytic action of Ag-NPs, the degradation of Methylene blue (MB) was used with the existence of UV light. Then 8 mg of Ag-NPs was added into 70 mL of MB solution (15 mg/L), while a control setup that did not contain any Ag-NPs was also checked. The suspension was stirred in dark for 30 min to be certain that the equilibrium of the working solution was prior to irradiation. After the suspension was prepared, it was placed under the UV-light, and had the deprivation of MB solution checked after every 20 min.

Results and discussion

UV–vis spectroscopy

The reduction of $AgNO_3$ to Ag-NPs through the employment of *S. leriifolia* aerial extracts was verified by determining the UV–Vis spectroscopy. $AgNO_3$ solution was added to the light brown aqueous aerial extract. The change of color towards dark red (after 1 h) confirmed the formation of Ag-NPs (Fig. 2), which was caused by the reduction of Ag^+ to Ag^0 that was due to the existence of various biomolecules in the aerial extract.

The absorption spectra of Ag-NPs are recorded and depicted in Fig. 3. The Ag-NPs have shown a specific absorption peak at 418 nm. This SPR peak is very

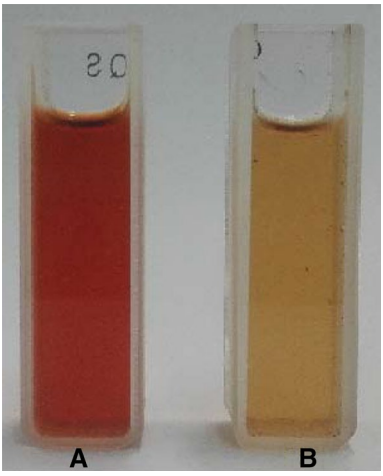

Fig. 2 The biologically synthesized Ag-NPs after 12 h (**a**) and the raw extract of *S. leriifolia* (**b**)

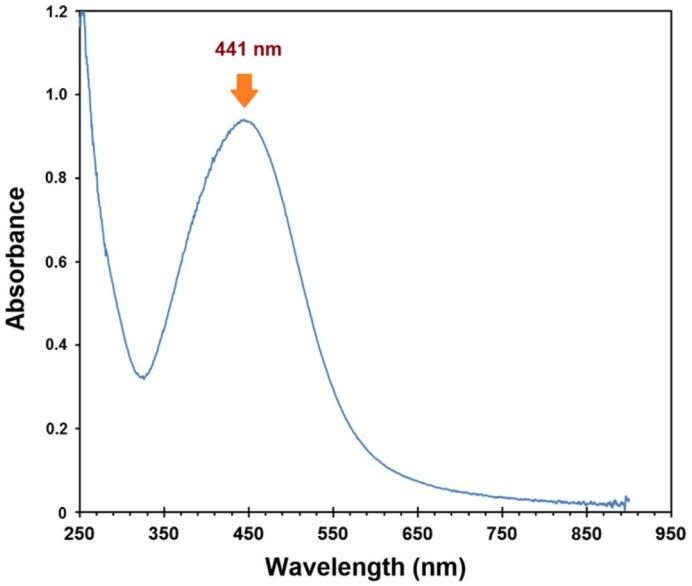

Fig. 3 The UV–vis spectrum of biosynthesized Ag-NPs in aqueous aerial parts extract of *S. leriifolia*

penetrating to the size and morphology of the nanoparticles, extent of plant-extract, $AgNO_3$ concentration and the type of bio-components that exist in the aerial extract. The spherical shape of the biosynthesized Ag-NPs has been verified with λ_{max} of 418 nm. Agreeing with work [28] in the UV–Vis spectrum, absorption bands in the range of 400–420 nm correspond to the spherical-shaped metallic nanoparticles.

TEM and FESEM images

The TEM images of Ag-NPs with high resolution is demonstrated in Fig. 4a, b. The image displays the spherical shape of the Ag-NPs (~ 12.8 nm) (Fig. 4c). Their surface morphology has been also tested through the FESEM images (Fig. 5) which have clearly revealed the small sizes and spherical morphology of our samples.

X-ray diffraction

The crystalline structure of biosynthesized Ag-NPs has been evaluated through the XRD studies. Figure 6 illustrates the PXRD pattern of Ag-NPs. The existence of distinctive peaks at 38.2, 44.6, 64.6, and 77.5 resemble the (111), (200), (220), and (311) indexing reflections, respectively. Accordingly, it matches so that the prepared Ag-NPs have faced centered cubic (fcc) structure, which is the Joint Committee on Powder Diffraction Standards (JCPDS) File No. 04-0783. The size of Ag-NPs obtained from the Scherrer equation (9.21 nm) was smaller than the mean particle size (12.78 nm) assessed by TEM images.

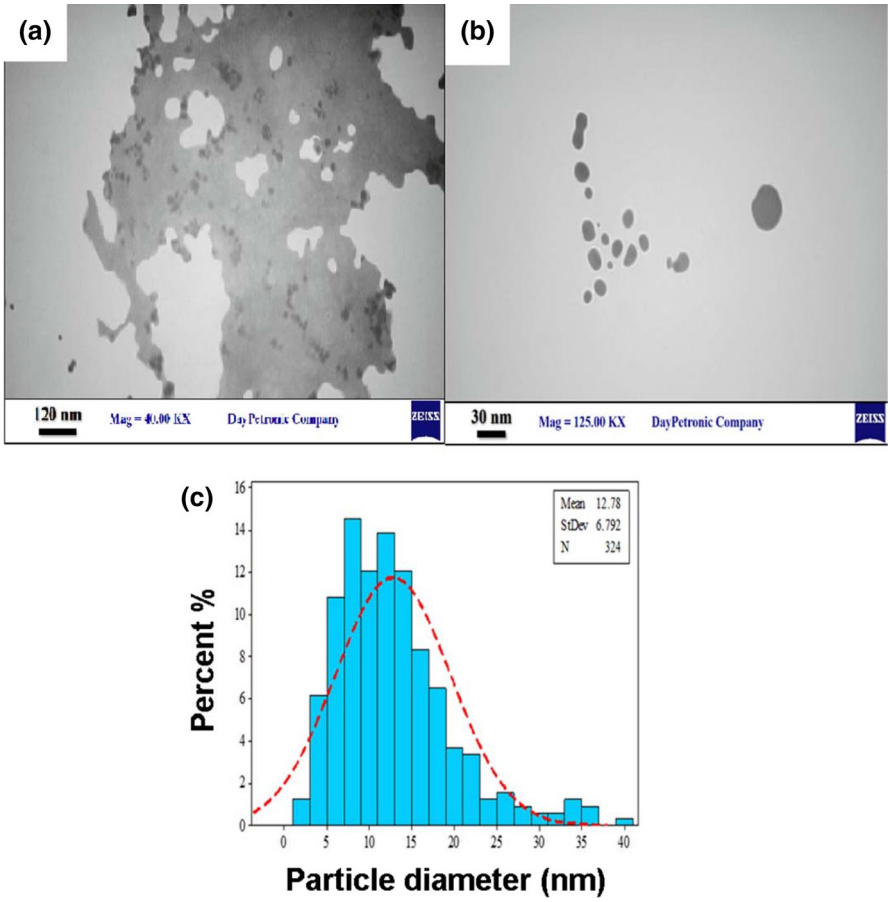

Fig. 4 High resolution TEM images of Ag-NPs in aqueous extract aerial parts of *S. leriifolia* (**a**) and its particles size distribution (**b**)

FT-IR spectroscopy

FTIR studies have been carried out to accomplish the objective of discovering various efficient clusters that are accountable for the formation of Ag-NPs. As displayed in Fig. 7, the FTIR result has shown specified peaks positioned at 603, 826, 1082, 1383, 1645, 2922, and 3330 cm^{-1}. The band at 603 cm^{-1} region could be attributed to the C–Br stretching, which is a characteristic of alkyl halides [29]. The band at 826 cm^{-1} seems to have been caused by the out-of-plane bending vibrations of a –O–H group [30]. The peak that has been observed at about 1082 cm can be related to the C–N stretching produced by the existing amines [18]. The characteristics bands at 1383 cm^{-1}, 1645 cm^{-1} and 2922 cm^{-1} are assigned to the nitro N–O bending, amide C=O and C–H stretching of alkanes, respectively [31, 32]. The peak at 1260 cm^{-1}, which is absent for the Ag-NPs FT-IR spectrum, can be ascribed to the

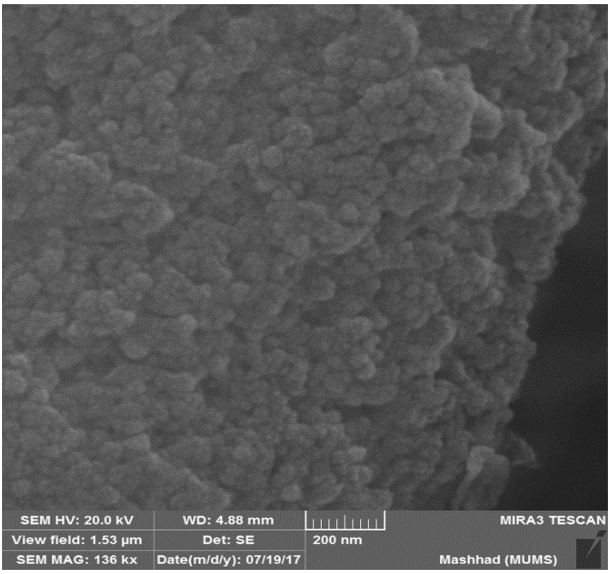

Fig. 5 FESEM image of prepared Ag-NPs in aqueous aerial parts extract of *S. leriifolia*

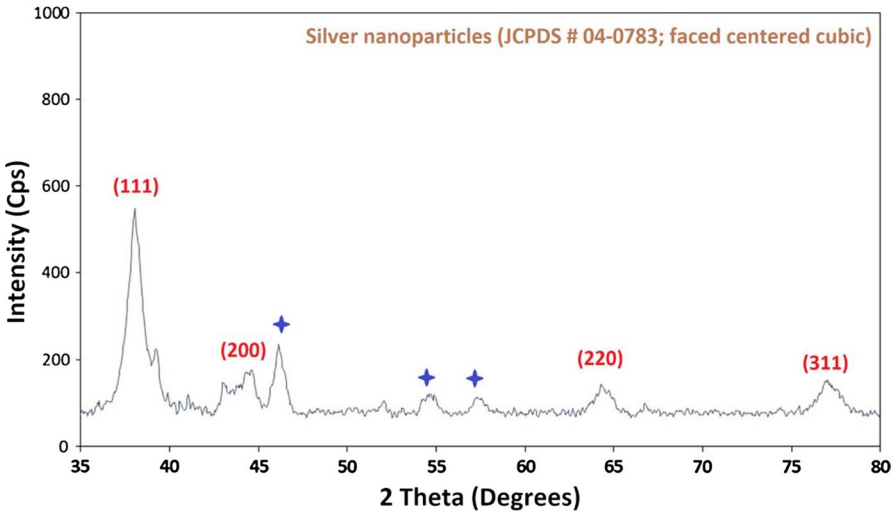

Fig. 6 The PXRD pattern of bio-synthesized Ag-NPs in aqueous aerial parts extract of *S. leriifolia*

S=O stretching vibration of the sulphated groups [33] and could be due to the stabilization of Ag-NPs through this group. Moreover, the band at 3330 cm^{-1} is probably allocated to the OH stretching of ascorbic, malic and citric acid. It is obvious that a red shift occurs during the synthesis process of Ag-NPs according to interaction between Ag^{+} ions or Ag-NPs with carboxylic functional groups in ascorbic, malic and citric acids [34].

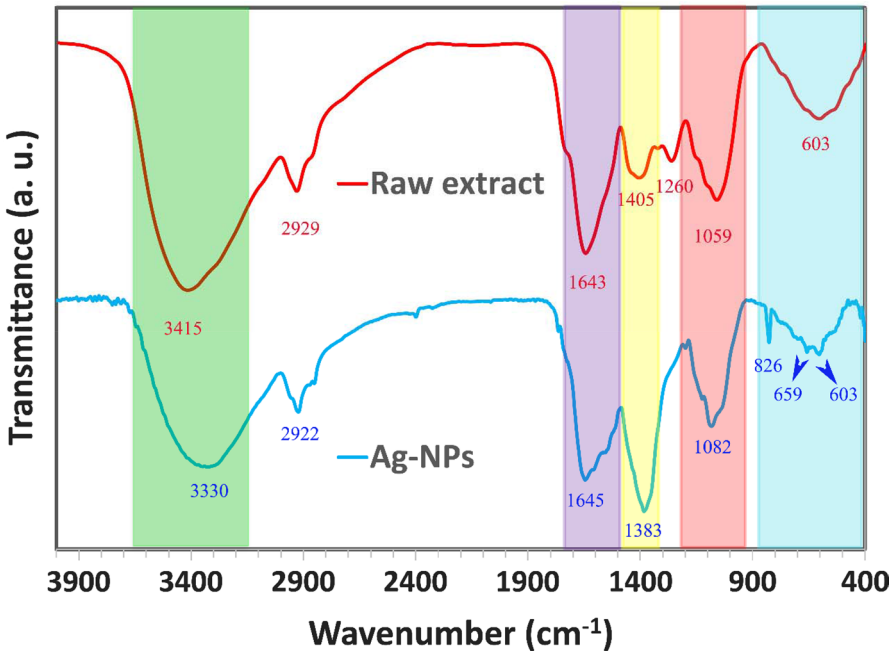

Fig. 7 The FTIR spectra of the raw extract and the prepared Ag-NPs in aqueous aerial extract of *S. leriifolia*

Determination of the Ag-NPs concentration

TEM images indicated that nanoparticles were shaped spherically, therefore, its concentration was approximated by applying the density of silver and the volume obtained from the mean diameter of the particle. Then, the mean particle weight could be measured through its relation with density and volume. In the next step, the particles were separated by centrifuge and weighted accordingly to prepare a 1000 ppm solution of Ag-NPs. Further suspensions were made from a 1000 ppm suspension.

Antibacterial tests

The well-known repressive effect of silver has been known and used for several curative uses. Therefore, the well diffusion method was employed to test the antibacterial properties of the Ag-NPs that have been biosynthesized by aerial parts of *S. leriifolia* extract (Fig. 8). Bacterial infections are a major cause of chronic infections and mortality. Antibiotics have been the favorite usage for bacterial infections because of their cost-effectiveness and great effects. Though, numerous studies have providing direct evidence that the widespread use of antibiotics has led to the emergence of multidrug-resistant bacterial strains. Different procedures have been proposed for

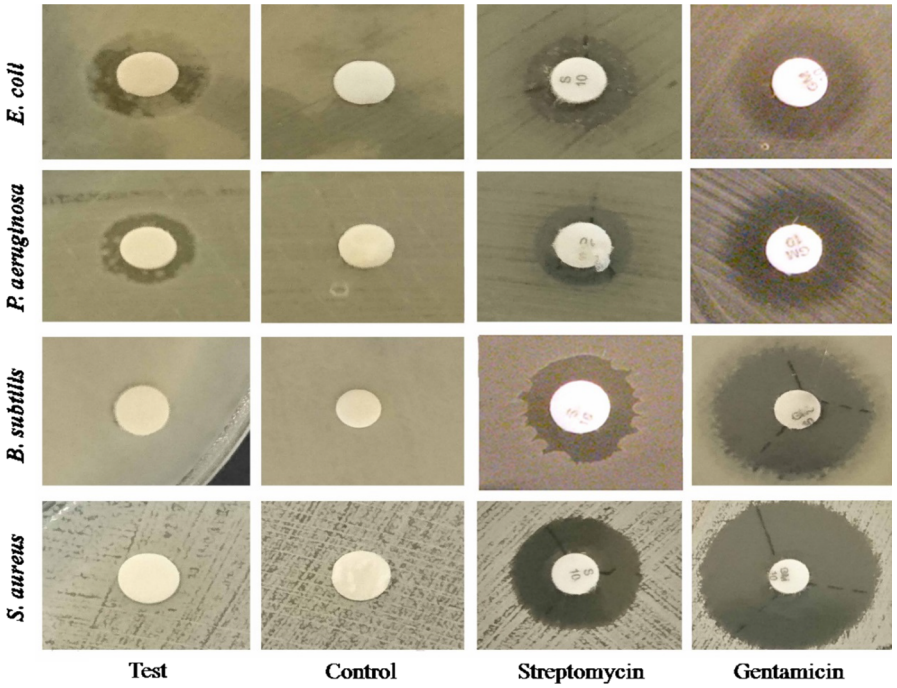

Fig. 8 Antibacterial activity of prepared Ag-NPs contrary to pathogenic bacteria by the disk-diffusion method

the antimicrobial effect of Ag-NPs. It has been reported that the cell-death might be due to the cytoplasmic membrane incompetence and the significant leakage of several bio-components (e.g., protein and carbohydrates) [35]. Furthermore, they have shown that the cell-death could have been caused by the inhibition of various essential enzymes [36]. The results of antibacterial tests show biosynthesized Ag-NPs from *S. leriifolia* extract have high potential against the most common pathogenic bacteria (Table 1).

Photo-degradation of MB

A global character of the human activity with respect to development of industry, the agroindustrial complex, and transportation poses the ecological problems as the most topical. The results of this study and the literature data indicate a suitable efficiency of photocatalytic methods in the degradation of stable and organic dye which is useful for degradation of pollutants such as industrial dyes in aquatic environments. During degradation the catalysis occurs on the surface region of metals, therefore increasing the surface area availability will significantly expand the efficacy of the catalyst [37]. Decreasing the particle size will increase the catalytic action, but there is a critical size below which proves that further decreases will actually hamper the reaction [38]. Metal nanoparticles provide the electron (e^-)

Table 1 Diameter regions of inhibition by Ag-NPs contrary to pathogenic bacteria

Bacteria	Inhibition zone (mm)			
	Test	Control negative	Control positive	
	Ag-NPs	Water	GM	S
E. coli	10.5	NA	15	11
P. aeruginosa	10	NA	16	11
B. subtilis	7.5	NA	25	18
S. aureus	9	NA	32	12

Mean standard deviation values for the *S. aureus* = ± 0.90 mm, *B. subtilis* = ± 0.10 mm, *E. coli* = ± .80 mm, *P. aeruginosa* = ± 0.70 mm for Ag-NPs

NA not appearing, *GM* gentamicin, *S* streptomycin

relay from the donor to the acceptor and act as a substrate for the e^- transfer reaction. During e^- transferal reaction, the reactants are adsorbed on the surface of the metal and therefore, the reactants gain an e^- and are reduced. Thus, Ag-NPs act as an efficient catalyst through the electron transfer manner in all the above catalytic reactions [39]. The high photo-catalytic efficiency of nanoparticles is of abundant importance for environmental aspects. Many different industries have released a variety of harmful compounds (dyes, organic materials) throughout the environment that have caused adversarial effects. MB is a stable organic compound that contains a large heterocyclic aromatic molecular structure [40] and is utilized in testing the photo-catalytic activity of Ag-NPs. The results have shown absorption peak decreases hastily with the existence of Ag-NPs and light, which indicates the photo-degradation of MB. Moreover, the degradation of MB seemed to be sluggish in the presence of Ag-NPs and the absence of light (Fig. 9).

Conclusion

We have synthesized the Ag-NPs using the aqueous aerial extract of *S. leriifolia* and characterized them using various techniques such as UV–visible spectrophotometry, FESEM, XRD, TEM, and FTIR. All the analyses confirmed the formation of Ag-NPs. UV–visible spectrophotometry showed an intense peak of silver nano-crystals at 418 nm. TEM images revealed homogeneous spherical shaped Ag-NPs with a size of ~ 12.8 nm. The FTIR analysis indicated that different biological components in plant extract such as phenols, amines; citric acid acted as reducing agents and caused the formation of Ag-NPs. The biosynthesized Ag-NPs show high antibacterial activity against pathogenic bacteria (both Gram-positive bacteria, i.e., *Staphylococcus aureus* and *Bacillus subtilis* and Gram-negative bacteria, i.e., *Escherichia coli* and *Pseudomonas aeruginosa*), especially against *E. coli* with an inhibition zone of 10.5 mm. Biosynthesized Ag-NPs indicated a photodegradable stable component (MB). Bacterial pollutions can occur from the propagation of pathogenic

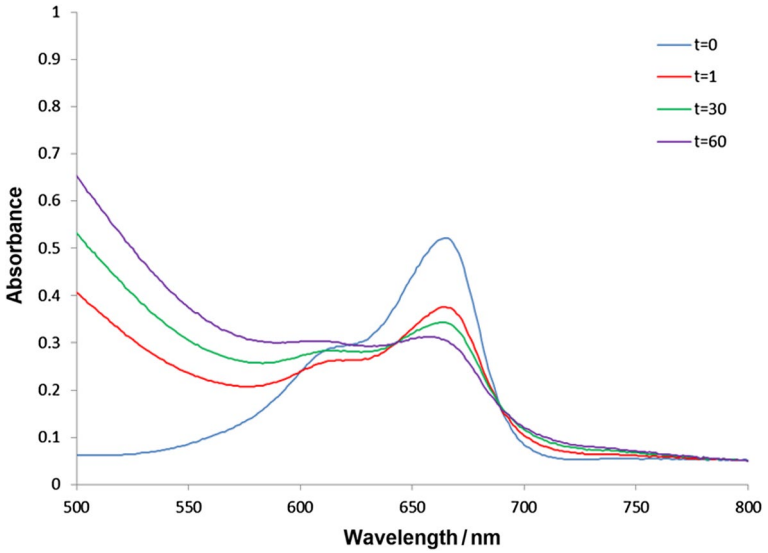

Fig. 9 Photo-degradation of MB in presence of biosynthesized Ag-NPs

bacteria and can cause pneumonia, urinary tract infections, and many other forms, that can cause damage and even death in some individuals. Bio-application of Ag-NPs shows they are suitable for medical instruments and infection disease. The large-scale production and widespread application of synthetic dyes can cause substantial environmental pollution, making it a serious public concern. Thus, the green synthesized nanoparticles have a crucial role and can be utilized for removal of sustained wastewater and sewage.

Acknowledgement The authors gratefully acknowledge the instrumental support from the Mashhad University of Medical Sciences and Farhangian University.

References

1. Z.U.H. Khan, A. Khan, Y. Chen, N.S. Shah, N. Muhammad, A.U. Khan, K. Tahir, F.U. Khan, B. Murtaza, S.U. Hassan, S.A. Qaisrani, P. Wan, J. Photochem. Photobiol. B **173**, 150 (2017)
2. A. Miri, M. Darroudi, R. Entezari, M. Sarani, Res. Chem. Intermed. **44**, 3169 (2018)
3. S. Goyal, N. Gupta, A. Kumar, S. Chatterjee, S. Nimesh, IET Nanobiotechnol. **12**, 526 (2018)
4. V. Kumar, R.K. Gundampati, D.K. Singh, M.V. Jagannadham, S. Sundar, S.H. Hasan, J. Ind. Eng. Chem. **37**, 224 (2016)
5. E. Abbasi, M. Milani, S. Fekri Aval, M. Kouhi, A. Akbarzadeh, H. Tayefi Nasrabadi, P. Nikasa, S.W. Joo, Y. Hanifehpour, K. Nejati-Koshki, Crit. Rev. Microbiol. **42**, 173 (2016)
6. V. Kumar, S. Mohan, D.K. Singh, D.K. Verma, V.K. Singh, S.H. Hasan, J. Mater. Sci. Eng. C. **71**, 1004 (2017)
7. S. Ahmed, M. Ahmad, B.L. Swami, S. Ikram, J. Adv. Res. **7**, 17 (2016)
8. V. Kumar, D. Bano, S. Mohan, D.K. Singh, S.H. Hasan, Mater. Lett. **181**, 371 (2016)
9. T.K. Das, S. Ganguly, P. Bhawal, S. Mondal, N.C. Das, Res. Chem. Intermed. **44**, 1189 (2018)
10. V. Kumar, D.K. Singh, S. Mohan, S.H. Hasan, J. Photochem. Photobiol. B **155**, 39 (2016)

11. E. E. Elemike, D. C. Onwudiwe, A. C. Ekennia, A. Jordaan. IET Nanobiotechnol., (2018)
12. V. Kumar, R.K. Gundampati, D.K. Singh, D. Bano, M.V. Jagannadham, S.H. Hasan, J. Photochem. Photobiol. B **162**, 374 (2016)
13. M. N. Gjerding, M. Pandey, K. S. Thygesen. Nat. Commun. **8**, (2017)
14. V. Kumar, D.K. Singh, S. Mohan, R.K. Gundampati, S.H. Hasan, J. Environ. Chem. Eng. **5**, 744 (2017)
15. A.M. Zaniewski, M. Schriver, J. Gloria Lee, M. Crommie, A. Zettl, Appl. Phys. Lett. **102**, 023108 (2013)
16. J. Ai, E. Biazar, M. Jafarpour, M. Montazeri, A. Majdi, S. Aminifard, M. Zafari, H.R. Akbari, H.G. Rad, Int. J. Nanomed. **6**, 1117 (2011)
17. K. Luyts, D. Napierska, B. Nemery, P.H. Hoet, Environ. Sci. Process. Impacts **15**, 23 (2013)
18. M.E.T. Yazdi, J. Khara, H.R. Sadeghnia, S.E. Bahabadi, M. Darroudi, Res. Chem. Intermed. **44**, 1325 (2018)
19. S. Iravani, Green Chem. **13**, 2638 (2011)
20. M. Modarres, S.E. Bahabadi, M.E.T. Yazdi, Cytotechnology **70**, 741 (2018)
21. V. Kumar, D.K. Singh, S. Mohan, D. Bano, R.K. Gundampati, S.H. Hasan, J. Photochem. Photobiol. B **168**, 67 (2017)
22. M. Mahdavi, F. Namvar, M.B. Ahmad, R. Mohamad, Molecules **18**, 5954 (2013)
23. J. Baharara, F. Namvar, T. Ramezani, M. Mousavi, R. Mohamad, Molecules **20**, 2693 (2015)
24. A. Balkrishna, N. Sharma, V.K. Sharma, N.D. Mishra, C.S. Joshi, IET Nanobiotechnol. **12**, 371 (2017)
25. S. Emami, F. Nadjafi, G. Amine, M. Amiri, M. Nasseri, M. Khosravi, J. Ethnopharmacol. **48**, 48 (2012)
26. M. Modarres, J. Asili, M. Lahouti, A. Gangali, M. Iranshahy, A. Sahebkar, J. Liq. Chromatogr. Relat. Technol. **37**, 1721 (2014)
27. K. Dovi, K. Yoel, R. Eugene, I. Micha, I. Ilan, L. Yossi, Aquat. Microb. Ecol. **24**, 9 (2001)
28. T. Prathna, N. Chandrasekaran, A.M. Raichur, A. Mukherjee, Colloids Surf. B **82**, 152 (2011)
29. K. Jyoti, M. Baunthiyal, A. Singh, J. Radiat. Res. Appl. Sci. **9**, 217 (2016)
30. P. Balashanmugam, P.T. Kalaichelvan, Int. J. Nanomed. **10**, 87 (2015)
31. S. Ahmed, M. Ahmad, B.L. Swami, S. Ikram, J. Radiat. Res. Appl. Sci. **9**, 1 (2016)
32. S. Ahmed, S. Ikram, J. Nanomed. Nanotechnol. **6**, 309 (2015)
33. L. Pereira, A.M. Amado, A.T. Critchley, F. Van de Velde, P.J. Ribeiro-Claro, Food Hydrocoll. **23**, 1903 (2009)
34. M. Bindhu, P.V. Rekha, T. Umamaheswari, M. Umadevi, Mater. Lett. **131**, 194 (2014)
35. R.S. Patil, M.R. Kokate, S.S. Kolekar, Spectrochim. Acta Part A **91**, 234 (2012)
36. C. Krishnaraj, E. Jagan, S. Rajasekar, P. Selvakumar, P. Kalaichelvan, N. Mohan, Colloids Surf. B **76**, 50 (2010)
37. S. Bhakya, S. Muthukrishnan, M. Sukumaran, M. Muthukumar, S.T. Kumar, M. Rao, J. Bioremediat. Biodegrad. **6**, 1 (2015)
38. C. Grogger, S. Fattakhov, V. Jouikov, M. Shulaeva, V. Reznik, Electrochim. Acta **49**, 3185 (2004)
39. P. Christopher, H. Xin, S. Linic, Nat. Chem. **3**, 467 (2011)
40. K. Tahir, S. Nazir, B. Li, A.U. Khan, Z.U.H. Khan, A. Ahmad, F.U. Khan, Sep. Purif. Technol. **150**, 316 (2015)